

## P11.3 HIGH RESOLUTION MOBILE MESONET OBSERVATIONS OF RFD SURGES IN THE JUNE 9 BASSETT, NEBRASKA SUPERCELL DURING PROJECT ANSWERS 2003

Catherine A. Finley\* and Bruce D. Lee

Sr. Atmospheric Scientists  
WindLogics, Inc.

### 1. INTRODUCTION

There are many unresolved issues regarding tornadogenesis in supercells. One question that has received recent attention in the research community is the role of the rear flank downdraft (RFD) and rear flank downdraft boundary (RFDB) in the tornadogenesis process. Project ANSWERS (Analysis of the Near-Surface Wind and Environment Along the Rear Flank of Supercells) 2003 was a field experiment designed to collect near-surface data in order to document the kinematic and thermodynamic environment in the vicinity of the RFDB, and to try to determine the RFD and RFDB's contribution to low-level mesocyclogenesis, tornadogenesis and tornado maintenance.

Approximately 12 different RFDs (both tornadic and nontornadic) were sampled by Project ANSWERS using an array of four mobile mesonet vehicles during the late spring and early summer of 2003. One case of particular interest occurred on June 9<sup>th</sup> near Bassett, Nebraska in which a weak tornado developed in very close proximity to the project's mobile mesonet. During the 10 minute period prior to tornadogenesis, the teams were deployed in a configuration such that high spatial resolution data could be collected in the RFD region of the storm. This ten minute period between 22:50 – 23:00 UTC will be the focus of this study.

### 2. JUNE 9, 2003 DATA COLLECTION AND ANALYSIS

Data was collected with an array of four mobile mesonet stations similar in design to those described by Straka et al. (1996) using updated versions of equipment wherever possible. Atmospheric variables were sampled every 2 seconds, and the data was quality controlled using criteria similar to Markowski et al. (2002) and bias corrected prior to analysis. Each variable sample was then averaged over a 12 second period to remove very small timescale fluctuations. Unless otherwise noted, all data plots shown for the June 9 case are averaged data. In addition to the measured atmospheric quantities, several derived variables were calculated including  $\Theta_v$  and  $\Theta_e$ , and departures of these variables from their prestorm

environment values ( $\Theta_v'$  and  $\Theta_e'$ ). Since surface observing stations are very widely spaced in northern Nebraska, pre-storm environment values were calculated from average mesonet measurements taken in front of the storm tens of minutes before storm intercept. Measured pressures were reduced to a common elevation (average elevation of the mesonet over a particular day) in order to remove pressure differences due to changes in elevation.

In order to try to gain some understanding of the two-dimensional structure in the RFD region of the storm, time-space conversion was applied in a manner similar to Markowski et al. (2002). In order to perform the time-space conversion, one must assume the storm is in 'steady-state' for some specified period of time. The position of the mesonets can then be plotted relative to the storm creating a quasi-2D view of the atmosphere. Since radar data was available every 5-6 minutes, time-space conversion was done over a five minute period with full appreciation that it was highly unlikely that the storm was in 'steady-state' for 5 minutes. Thus, as one views data points further from the center time of the time-space conversion, the analyzed fields become less certain. Storm motion for the time-space conversion was calculated from the average motion of the mid-level mesocyclone (as identified in the KLNx radar reflectivity field) over a 15 minute period from 22:50 – 23:05 UTC.

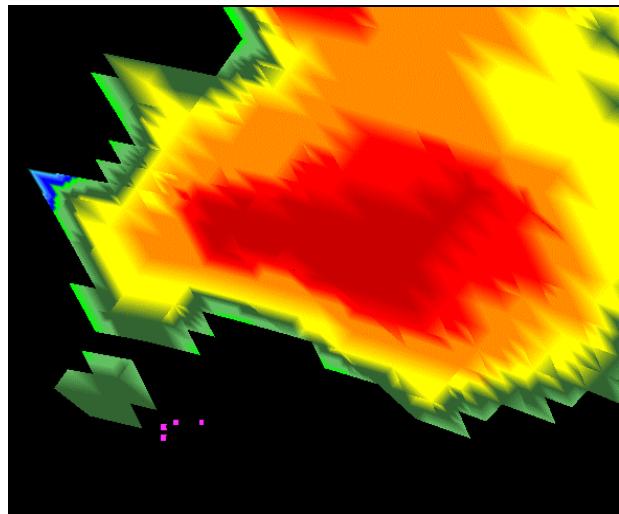


Fig. 1. Radar reflectivity at 22:50 UTC at the lowest elevation scan from the KLNx radar. The positions of the four mesonet teams at this time are depicted by the pink dots.

\* Corresponding author address: Dr. Cathy Finley, Windlogics, Inc., Itasca Technology Center, 201 NW 4<sup>th</sup> Street, Grand Rapids, MN 55744  
email: cfinley@windlogics.com

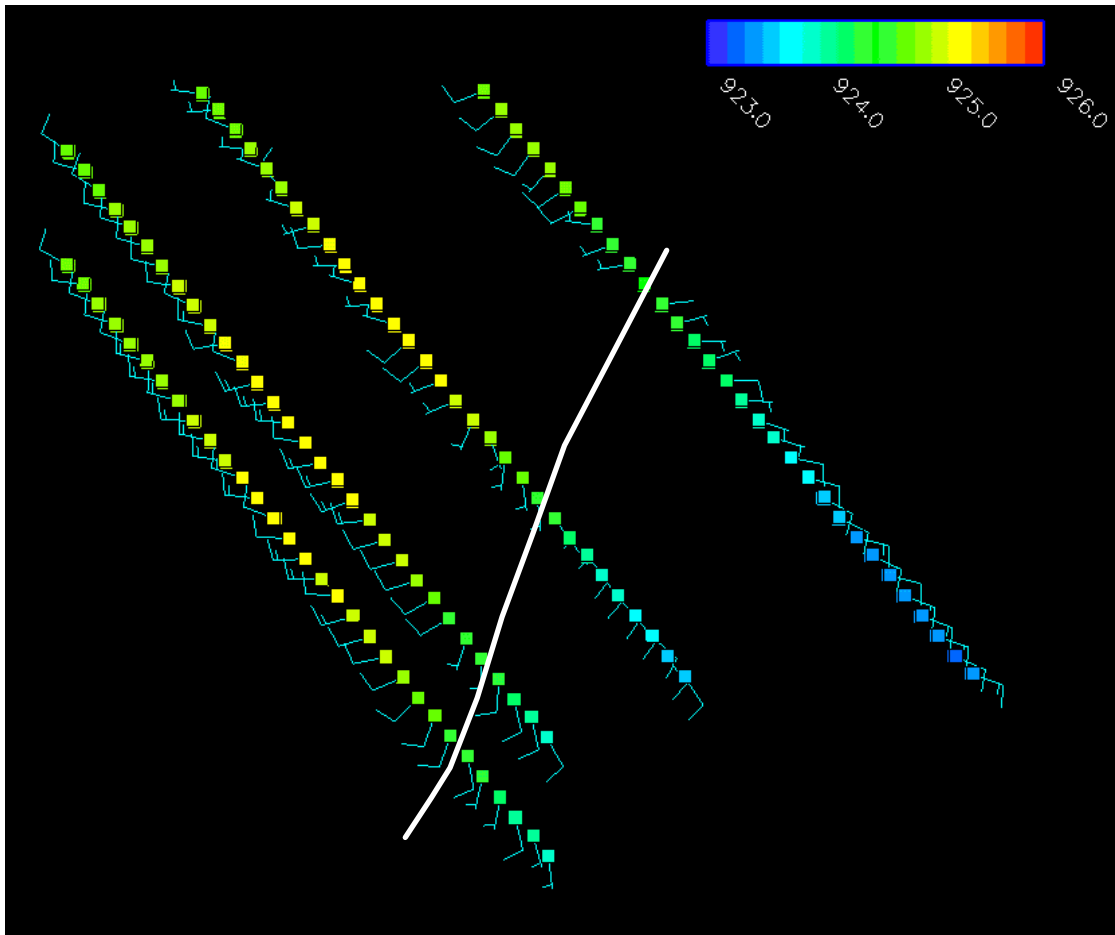


Fig. 2: Time-space conversion over a 5 minute period centered at 22:50 UTC. Mesonet data is plotted every 10 s. The wind barbs depict the ground-relative wind in knots. The color on the mesonet positions shows the measured pressure in mb reduced to a common elevation (scale shown in upper right corner). The white line depicts the position of the first RFD boundary. The storm (not shown) is approaching the mesonet array from the northwest. Mesonet identifiers (from left to right) are M4, M3, M2, and M1.

The target storm developed at the intersection between a warm front and dry line in north-central Nebraska. Project ANSWERS intercepted the storm at approximately 21 UTC (very early in its life) north of Bassett, NE. Due to the poor road network, it was decided to deploy the teams at fixed locations and let the storm approach and pass over the mesonet array from the northwest. Additional data was collected on several RFDs on this day (both tornadic and nontornadic) as this storm went on to cycle many times producing an F0 tornado northeast of Bassett, an F1 tornado near Stuart, NE, and an F3 tornado just north of O'Neil, NE (after a storm merger).

### 3. RESULTS

All teams came to a stop in their final positions for this event shortly before 22:48 UTC. Visually the storm looked like a small LP supercell with a rotating wall cloud to the N/NW of the mesonets. The first RFD

boundary was weak and passed over the mesonet array between 22:48:30-22:51:00 UTC as shown in Figure 2. The passage of this boundary was marked by a shift in the winds from S/SE to W. All teams recorded a ~1.5 mb pressure rise following the passage of the boundary, with no noticeable change in temperature.  $\Theta_v'$  values were generally -1 K behind the boundary.

A second RFD surge began to pass over the mesonet array starting at ~ 22:54:40 UTC with the storm-relative winds at M3 turning around to the NW and increasing from < 5 kts to 15 kts (see Figure 3). This surge is marked by a slight cooling ( $\Theta_v'$  values decrease by ~0.5 K at M2, M3, and M4 locations) and a pressure fall of about 0.5 mb (not shown). Despite the slight cooling, the air in the RFD was still quite warm with  $\Theta_v'$  values only 2 K cooler than the environment. During this second surge, positive vertical vorticity  $\sim 0.01\text{-}0.015\text{ s}^{-1}$  develop on the north side of the surge between M2 and M3. Between 22:55:20 – 22:57:30 UTC a small vortex forms along the cyclonic side of the

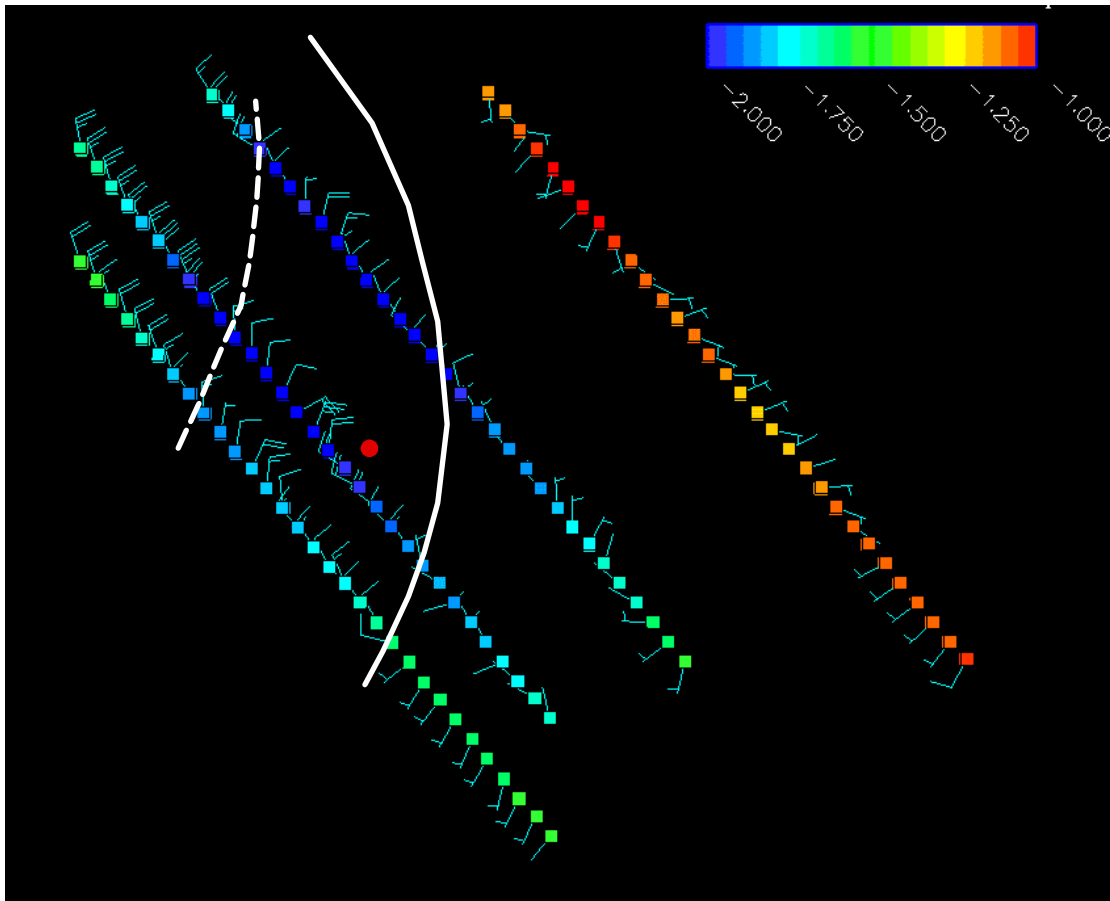


Fig. 3: Time-space conversion over a 5 minute period centered at 22:56 UTC. Mesonet data is plotted every 10 s. The wind barbs depict the storm-relative wind in knots. The color on the mesonet positions shows the value of  $\Theta_v'$  in degrees Kelvin (scale in the upper right corner). The solid white line depicts the position of the second RFD surge boundary. The dashed white line depicts the position of a possible third RFD boundary. The shearing instability which develops east/northeast of M3 is depicted with a small red dot.

RFD just E/NE of M3, depicted by the small red dot in Figure 3. This small vortex did not spin up to tornadic strength and was most likely a 'gustnado' or shearing instability as several small vortices were seen to the west of M1 at this time along the cyclonic side of the RFD as shown in Figure 4. M3 experienced a 0.5 mb pressure drop associated with the passage of this feature. Note that by 22:58:30 UTC (the last points plotted in Figure 3 in the upper left corner), M1 is not yet in the RFD surge although M2 just 1 km to the west has been in the RFD surge for several minutes. During this time period, strong rotation was also seen at cloud base immediately north of M1 and M2.

A potential third RFD surge occurs at ~22:55 UTC (and continues until the end of the analysis period) with the winds backing again to the NW and speeds increasing at M2-M4 locations (indicated by the dotted line on Figure 3). This is labeled as a 'potential' RFD surge because it is not completely clear if this is a new RFD surge, or a 'recovery' of the previous RFD from the shearing instabilities near the leading edge.

Nevertheless, the winds increase markedly, and the cyclonic/anticyclonic vortex sheets to the north/south of M3 are again established with positive vertical vorticity values  $\sim 0.01-0.025 \text{ s}^{-1}$  on the north side of the surge between M2 and M3 (and between M2 and M1), and anticyclonic vertical vorticity  $\sim 0.01-0.025 \text{ s}^{-1}$  along the south side of the surge between M3 and M4. Note that the  $\Theta_v'$  values begin to increase behind the third RFD surge.

The wind speeds at M1 increased to sustained values over 35 kts with a peak instantaneous value of 43 kts at  $\sim 23:00:50$  UTC as a weak tornadic vortex developed just to the north/northeast of M1 as shown in Figure 6 (M1 experienced a glancing blow from this vortex). If the boundary of the second/third RFD is extrapolated northward, it appears the vortex developed along the northern periphery of the second/third RFD surge along the strong cyclonic vortex sheet. M1 experienced a 1.5 mb pressure drop associated with this feature. Visually the vortex appeared to develop near the surface (no funnel clouds were visible prior to



Fig. 4. Picture taken from M1's location at ~22:56 UTC looking west-southwest. Several 'gustnados' or shearing instabilities can be seen, along with a general area of dust lofted by the RFD.

its formation), although very strong rotation was visible at cloud base just north of M1 immediately preceding tornadogenesis. The vortex (which was officially reported as a tornado by other chase groups in the area) was characterized by a broad circulation with multiple vortices embedded within it as shown in Figure 5. A small funnel at cloud base was visible for a short time period and did appear to be connected with the surface circulation.

The positions of the mesonet teams relative to the storm at the time of tornadogenesis are shown in Figure 7. All teams were deployed in the RFD region with M1 positioned ~1.5 km southwest of the mid-level mesocyclone as depicted in the reflectivity field. No well-defined mid-level mesocyclone could be discerned in the KLNx Doppler velocity fields until the 23:05 UTC scan. It should be noted that none of the mesonet teams experienced any precipitation during this first tornado cycle, although precipitation was encountered ~5 minutes later as the teams moved east to reposition for another deployment. Following the passage of the tornadic vortex, all teams (including M1) were in a divergent RFD for several minutes.

#### 4. SUMMARY AND DISCUSSION

We have presented some preliminary analysis of the high-resolution mobile mesonet data collected in the RFD region of a tornadic supercell near Bassett, Nebraska on June 9, 2003. Four mesonet teams collected high spatial resolution data in the RFD region during the first tornadic cycle of this storm.

During the first tornadic cycle, as many as 3 RFD surges occurred in the 10 minute period preceding tornadogenesis. Although  $\Theta_v'$  varied somewhat between RFD surges, it was never more than 2.3 K cooler than

the environment at any of the mesonet locations, indicating that the RFD surges were relatively warm. Following the third RFD surge,  $\Theta_v'$  increased with  $\Theta_v'$  deficits approaching values of approximately -1 K as the mesonet position got further into RFD core.

Kinematically, the second and third RFD boundaries were very different than the first. The first RFD boundary was weak with the winds slowly veering from south/southeast to west during the passage of the boundary. The second and third surges exhibited a narrow 'spearhead' RFD structure with cyclonic/anticyclonic vorticity sheets to the north/south of the RFD core. Vertical vorticity values as large as  $\pm 0.025 \text{ s}^{-1}$  were calculated along the north/south sides of the RFD surge. Using M3's position as the center point of the RFD and assuming symmetry about the center point, the width of the second/third RFD surges are estimated to be only 2–3 km wide in this case.



Fig. 5. Photographs taken of the tornadic vortex ~ 1 minute after tornadogenesis. The top panel shows the view from M1 looking east (photo by Bruce Lee) and the bottom panel shows the view looking east from M2 (photo by Matt Grzych). The multiple vortex structure is clearly visible in the bottom photo.

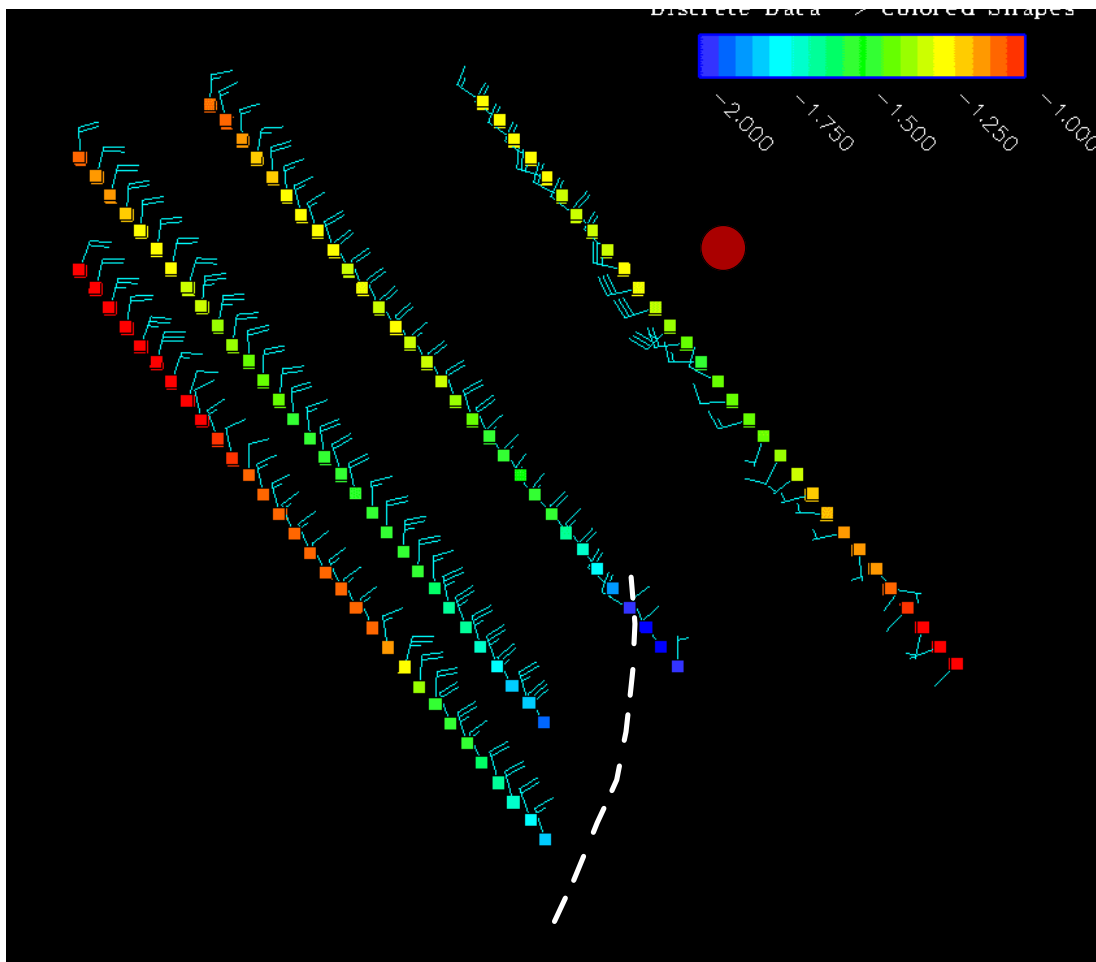


Fig. 6: As in Fig. 3 but at 23:00 UTC. The large red dot shows the approximate position of the tornadic circulation which developed just north of M1.

Several shearing instabilities were seen (both visually and in the mesonet data) in the cyclonic shear region of the second RFD surge. The tornadic circulation also developed in the cyclonic shear region of the second/third RFD surge suggesting that the tornado could have developed from a shearing instability. Model simulations of tornadic supercells (Finley et al. 2002) and some high resolution radar observations (Matt Gilmore, personal communication) have shown that shearing instabilities can move north/northwestward along the RFD boundary into the strong convergence beneath the mesocyclone, suggestive of a possible link between these shearing instabilities and tornadogenesis. The mesonet data suggests that a shearing instability may have passed by M2 ~1 minute after one moved by M3/M4 (see Figure 5). However, it is not clear that the low-level wind field in this case supports advection of shearing instabilities to the north along the RFD boundary (the storm-relative winds in front of the boundary are weak). Further analysis is underway to construct vorticity budgets in this case in order to shed more light on the tornadogenesis process.

## 5. ACKNOWLEDGEMENTS

This research was supported by the National Science Foundation under grants ATM-0105279 and ATM-0432408. Matt Grzych is acknowledged for his help in constructing the UNC mesonet stations. All participants of Project ANSWERS are thanked for their contributions to the data collection. Pat Skinner, Erik Crosman, and Bryan Guarente are recognized for their work on the quality control of the mesonet data and project operations support. We would also like to thank Dennis Moon for his assistance in getting the radar and mesonet data into the Environmental Workbench format.

## 6. REFERENCES

- Finley, C.A., W.R. Cotton, and R.A. Pielke, 2002: Tornadogenesis in a simulated HP supercell. *Preprints, 21<sup>st</sup> Conference on Severe Local Storms*, San Antonio, Amer. Meteor. Soc., 531-534.

Markowski, P. M., J. M. Straka, and E. N. Rasmussen, 2002: Direct surface thermodynamic observations within rear-flank downdrafts of non-tornadic and tornadic supercells. *Mon. Wea. Rev.* **130**, 1692-1721.

Straka, J. M., E. N. Rasmussen, and S. E. Fredrickson, 1996: A mobile mesonet for fine-scale meteorological observations. *J. Atmos. Oceanic Technol.*, **13**, 921-936.

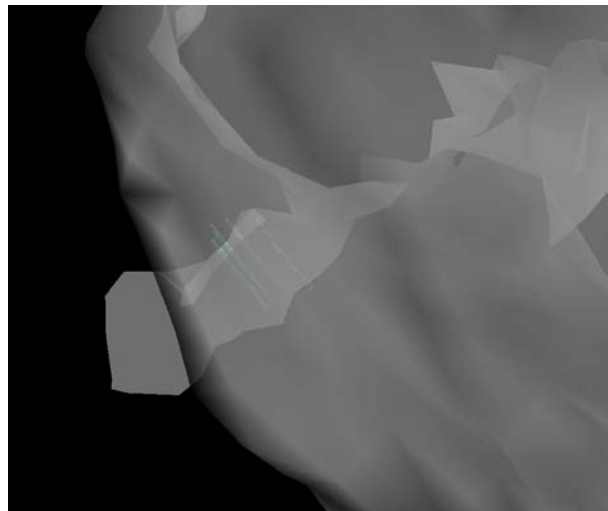
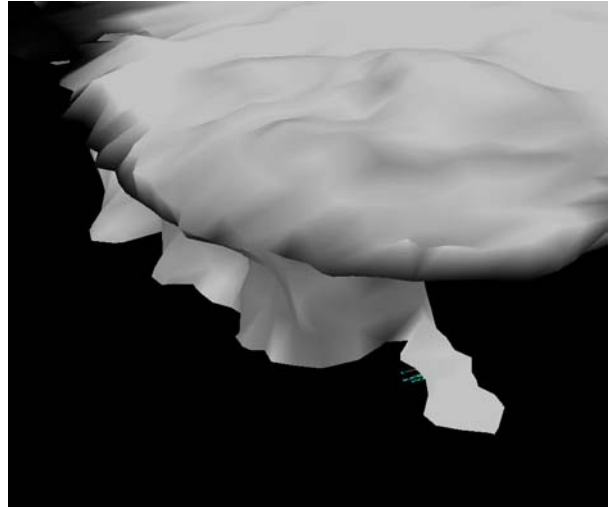


Fig. 7. Position of the mesonet teams relative to the storm at the time of tornadogenesis (23:00 UTC). At this time the storm was ~150 km away from the radar. The isosurface depicts the 24 dBZ value from the KLNK radar at 23:00 UTC. The top panel shows a view from the southwest (looking NE). The exact mesonet positions at this time are beneath flanking line. The bottom panel shows a top down view (with the reflectivity isosurface made somewhat transparent) of the mesonet positions plotted relative to the storm over a five minute period centered at 23:00 UTC.